Dense 3-D surface acquisition by structured light using off-the-shelf components

Jens Gühring*
Institute for Photogrammetry
University of Stuttgart/Germany

ABSTRACT

This paper describes the implementation of a LCD stripe projection system, based on a new processing scheme called line shift processing. One advantage of the method is, that the projection device can, but is not required to be stable over time nor does it have to be calibrated. The new method therefore allows us to use an off-the-shelf multimedia projector to acquire dense 3-D data (several 100K Triangles) of large objects in a matter of seconds. Since we are able to control our source of illumination, we can also acquire registered color information using standard monochrome cameras.

Besides the description of the system some practical examples are given. The calibration of the system is also addressed.

Keywords: Calibration, Inspection, Structured Light, 3-D Measurement System, Line Shift Processing

1. INTRODUCTION

Traditionally, coordinate measurement machines (CMMs) were used for 3-D mechanical part inspection. CMMs are well established and widely accepted in industry, but suffer from limitations such as high cost and low measurement speed. Therefore a number of different shape acquisition methods have been developed for a wide range of applications, including inspection, reverse engineering, digitization of virtual reality models and medicine.

Optical 3-D sensors measure the shape of objects without the need to physically probe surfaces. They are faster, cheaper and provide a higher measurement density than conventional techniques. One of the most popular approaches is optical triangulation. Particularly the class of active optical triangulation sensors provides dense and reliable surface acquisition by illuminating the scene rather than relying on natural or uncontrolled lighting.

Based on our experience in modeling, calibration and data processing of a commercial stripe projection system[2], we have developed a system that combines standard monochrome cameras with an off-the-shelf multimedia projector to form a flexible and efficient shape acquisition system.

The issues that are addressed in this paper are:

- the physical setup of the measurement system,
- the structure of the projected patterns,
- the data processing steps to convert the acquired images into 3-D surface measurements,
- calibration aspects and the
- practical performance of the entire system.

The remainder of this paper is organized as follows. We first describe our hardware setup in Section 2. Section 3 details the line shift method and the steps we use to reconstruct the 3-D shape of objects. The issue of calibration is addressed in Section 4. In Section 5 experimental results are given and Section 6 summarizes the results we have obtained.

* Correspondence: Email: jens.guehring@ifp.uni-stuttgart.de; WWW: http://www.ifp.uni-stuttgart.de/private/guehring

2. PHYSICAL SETUP FOR DENSE 3-D SURFACE ACQUISITION

2.1. Classification of Triangulation based Sensors

Dense surface acquisition is one of the most challenging tasks in computer vision. Active research in the last two decades led to a variety of high speed and high precision sensors including stereo camera systems, laser range finders and stripe projection systems.

The class of triangulation based sensors observes the object from at least two different angles. In order to obtain three-dimensional measurements, point correspondences have to be established, allowing 3-D shape to be reconstructed in a way that is analogous to the way the human eye works. The main difficulty is to come up with efficient solutions to solve this so called *correspondence problem*.

The family of triangulating sensors can be further subdivided in *active* and *passive* triangulation systems. *Active* triangulation systems illuminate the scene rather than relying on natural or uncontrolled lighting.

A stereo camera is the prime example of *passive optical triangulation.* For stereo vision, two or more cameras are used to view a scene. Determining the correspondences between left and right view by means of *image matching*, however, is a slow process. For faithful 3-D reconstruction of objects, *passive* stereo vision techniques depend heavily on cooperative surfaces, mainly on the *presence of surface texture*. The fact that most industrial parts lack this feature reduces its usefulness in an industrial context. However, since the underlying measurement principle is strictly *photogrammetric*, those methods enjoy all the advantages of *photogrammetric* systems, like the possibility for multiple observations (geometrically constrained matching), self-calibration, robustness and self diagnosis.

To overcome the need for cooperative surfaces and to speed up the evaluation steps, *active triangulation systems* project specific light patterns onto the object. The light patterns are distorted by the object surface. These distorted patterns are observed by at least one camera and then used to reconstruct the objects surface.

Some of the most widely used *active triangulation techniques* are:

- Light dot range finders: A single laser point is projected onto the surface and observed by a camera. If the position and orientation of the light source are known, a single 3-D point can be computed by intersection. For dense surface measurement, the light-dot must scan the surface.

- Light stripe range finders: A single line, usually a laser beam, spread by a cylindrical lens, is projected onto the objects surface. The resulting contour is detected by a camera and used to precisely calculate a three dimensional profile. If the light-stripe sweeps across the object, dense surface data is obtained. Due to their robustness and simplicity, light stripe range finders are very popular. A positioning device is needed to sweep the light stripe across the surface. The overall accuracy is affected by the accuracy of the positioning device.

- LCD shutter devices: A light projector shining through a computer controlled LCD screen is used to illuminate a surface in much the same way as in light-stripe range finder systems. The LCD effectively allows the surface to be scanned without needing to move the object. LCD shutter devices are suitable for measuring stationary objects, and are generally faster than light stripe systems for this type of task. Depth of field issues, however, make LCD devices less robust than light stripe devices.

- Slide projectors: The patterns are generated by switching glass slides, rather than relying on a re-programmable LCD. These slides are almost free of thermal expansion and can be fabricated very precisely. Slide projectors can achieve a contrast of more than 1:100. Due to the small slide size, an outstanding depth of field can be realized. The disadvantages are high costs, a fixed pattern design and effects arising from mechanical misalignment of the moving parts.

- Moiré devices: A set of fringe patterns is projected using an interference technique. The contours of the fringes are used to reconstruct the object's surface. Moiré devices are appropriate for the precise acquisition of smooth surfaces with few discontinuities.

2.2. Sensor Architecture

Our measurement system consists of a XGA multimedia projector, two or more monochrome cameras, a 3-axis positioning unit to place the object or the calibration plate in front of the sensor, a notebook computer to generate the stripe patterns and a PC to control the system and process the data (Figure 1). For our experiments we used a LCD type projector (Kindermann CPD Omega XV) as well as a DMD type projector (DAVIS DLX 650), both featuring high light output and a resolution of 1024×768 pixels, leading to comparably good results[4].

The connection between the PC and the notebook is established via TCP/IP using the OMG middleware platform CORBA. We use the OpenSource implementation MICO[4], a freely available and fully compliant implementation of the CORBA standard. The notebook is running a display server that can be controlled by the PC. The projection system is linked to the processing software in a transparent way, i.e. it can be replaced by any other projection device e.g. a commercially available stripe projector.

To acquire image data, we are using two or three digital cameras (Basler A113) with 2/3" imagers, $6.7\,\mu m$ pixel size at 1296×1024 pixels and $12\,mm$ Schneider-Kreuznach lenses. The cameras are mounted on a stable aluminum profile with a fixed, but unknown, relative orientation (Figure 1 (f)).

It has to be noted that in contrast to using a specialized stripe projector, which is more stable over time, only the cameras are calibrated. In this setup, the projector is only used as an aid to establish point correspondences.

Our system can be categorized as LCD shutter device in the taxonomy above. Compared to the techniques that sweep a single laser line or point over the surface, this setup has the advantage that there are no moving parts involved. Since all pixels can be addressed individually, arbitrary horizontal and vertical stripe patterns can be generated.

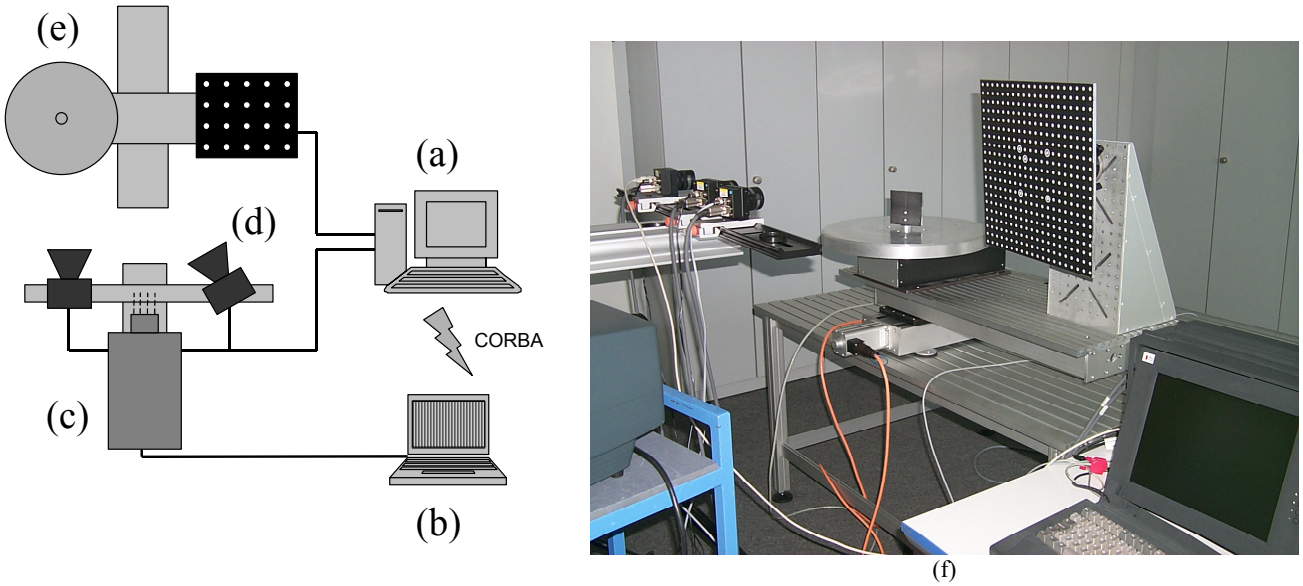

(f)

Figure 1: Set up of the measurement system: (a) PC for control and data processing; (b) notebook computer to generate stripe patterns; (c) multimedia projector; (d) cameras; (e) 3-axis positioning device to position either the object or the calibration plate.
(f) Photograph of the measurement system.

3. CODED LIGHT TECHNIQUES

3.1. Introduction to Coded Light Techniques

In light sectioning using light stripe range finders, a single line is projected onto the object (Figure 2 (a)) and then observed by a camera from another viewpoint. Tracking the bright line appearing in the image will yield all parallaxes and thus object depth along the profile. To recover the object's 3-D geometry, many lines have to be projected under different angles (Figure 2 (b)), which can be accomplished either by projecting an array of parallel lines simultaneously or by projecting different lines in temporal succession.

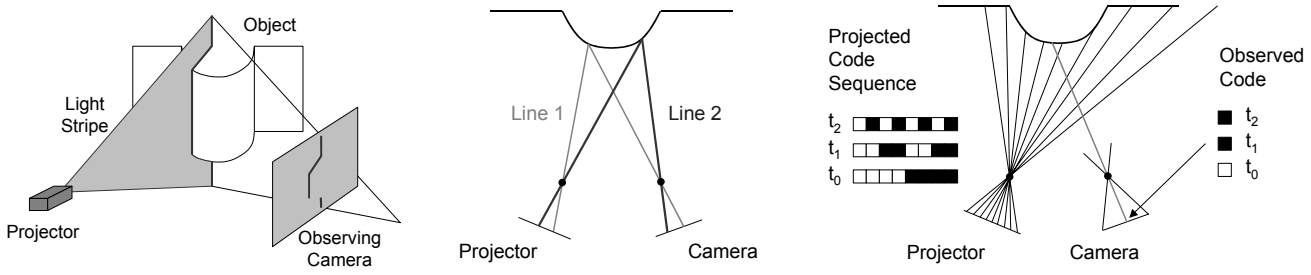

(a) (b) (c)

Figure 2. (a) Standard light sectioning with one light stripe. (b) Top view of light sectioning using more than one stripe. (c) Light sectioning using structured light.

The first method has the disadvantage that the lines have to be projected closely for a dense reconstruction. In this case, a ambiguity problem arises, especially at steep surfaces or jump edges. Projecting in temporal succession means that for n different light section angles n images have to be acquired, where n may be in the order of several hundreds to thousands.

This problem can be elegantly solved by the use of *coded light techniques*, which require only in the order of $\mathrm{ld}\, n$ images to resolve n different angles (see Figure 2 (c) for $n = 8$). Rather than projecting a single line per image, a binary pattern is used. This technique has been initially proposed by Altschuler et al.[1,2].

3.2. Solutions to the Correspondence Problem

3.2.1. Projection of Gray Code

For structured light analysis, projecting a Gray code is superior to a binary code projection (see Figure 3, top). On the one hand, successive numbers of the Gray code vary exactly in one bit. Thus, wrong decoding which is most likely to occur at locations where one bit switches, introduces only a misplacement of at most one resolution unit. On the other hand, the width of bright and dark lines in the pattern with finest resolution is twice as wide compared to the binary code. This facilitates analysis especially at steep object surfaces where the code appears to be compressed. Since we make use of a per pixel varying threshold, the Gray code solution is very robust. However, the resolution is limited to half the size of the finest pattern.

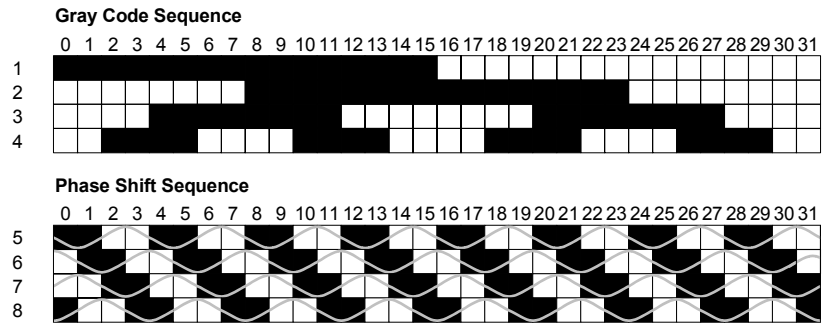

Figure 3. Gray code (top) and Phase Shift (bottom) of a $n = 32$ stripe code sequence.

3.2.2. Combination of Gray Code and Phase Shift

To obtain a resolution beyond the number of lines which can be switched by the projector it is very common to apply phase shifting. This uses the on/off intensity pattern generated by the switched projector lines as an approximation of a sine wave. The pattern is then shifted in steps of $\pi/2$ for a total of $N = 4$ pattern positions. Approximating the sampled values $f(\phi_i)$ at a certain fixed position (Figure 3, bottom) by

$$\begin{aligned} C \cdot \cos(\phi - \phi_0) &= C \cdot \cos\phi_0 \cos\phi + C \cdot \sin\phi_0 \sin\phi \\ &= A \cdot \cos\phi + B \cdot \sin\phi \end{aligned} \tag{1}$$

where the coefficients A and B can be determined from Fourier analysis by

$$A = \frac{2}{N}\sum_{i=0}^{N-1} f(\phi_i)\cos\phi_i \quad \text{and} \quad B = \frac{2}{N}\sum_{i=0}^{N-1} f(\phi_i)\sin\phi_i \ . \tag{2}$$

A phase shift $\phi_0 = \tan^{-1}(B/A)$ is obtained, which in our case ($N = 4$, $\phi_i = \{0, \pi/2, \pi, 3\pi, 3\pi/2\}$) simplifies to

$$\phi_0 = \tan^{-1}\frac{f_1 - f_3}{f_0 - f_2} . \tag{3}$$

However, it has to be taken into account that non-uniform object surface properties, such as a sharp change from black to white result in systematic measurement errors. Also, since the camera pixels effectively integrate over a certain area of the stripe code, the above error estimation is only true with a camera resolution sufficiently higher than the projector resolution.

Another problem arises if we want to combine measurements from different cameras using the same projector. The phase shift method yields for each camera pixel the corresponding projector stripe number with sub stripe accuracy. This means there is no direct link between image coordinates acquired by different cameras which is necessary to build a system with an uncalibrated projector.

3.2.3. Line Shift Processing

As a result of the insufficiencies of conventional phase shift processing, a detailed analysis of all requirements for the design of our new method has been performed.

We identified the following requirements, all of which have not been met by the conventional phase shift method:

- Ability for automation: The system should be able to adapt automatically to different objects without user interaction.
- Efficiency: Dense surface measurements of some 100.000 surface points should be feasible within a couple of seconds.
- Versatility: The method should extend over a wide range of sensor configurations, particularly the combination of multiple cameras with a calibrated or uncalibrated projector.
- Insensitivity to reflectance properties of object surface: Changes in surface reflectance should not cause systematic errors in range measurement.
- Accuracy information for 3-D coordinates: In addition to the object point coordinates, statistical measures for the quality of point determination should be available and used by further processing steps.
- Consistency and reliability: The system should prefer consistent and reliable points over complete coverage of the objects surface, especially in the presence of unfavorable lighting conditions and reflective surfaces.

To meet the formulated requirements, we have developed a new method, called *line shift processing*, to solve the correspondence problem fast and precisely.

As before, efficiency is achieved by making use of the highly parallel nature of our projection unit. However, the inherent problems in phase shift measurements made us to create a new pattern design. Thus, we have replaced the phase shift patterns by a sequence of parallel lines, achieved by illuminating each n^{th} projector line. For our experiments, we have chosen $n = 6$.

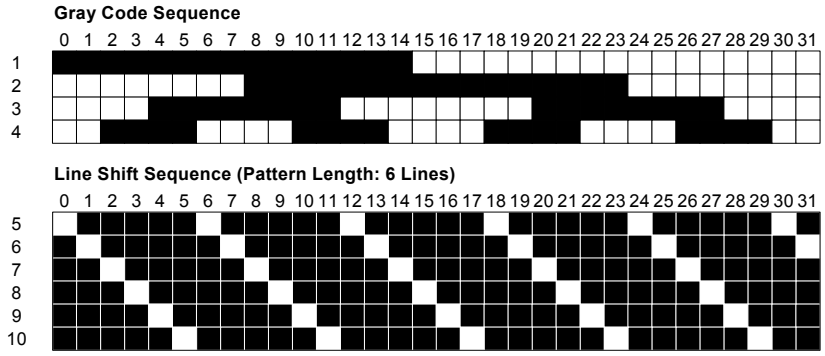

Figure 4. Gray code (top) and Line Shift (bottom) of a $n = 32$ stripe code sequence.

The evaluation of the so called line shift images is performed similar to the images obtained with a *light stripe range finder* (Section 2 and Figure 8). Six images for the *x* and six images for the *y* coordinates are needed to use the whole resolution provided by the projector. First, the line centers are detected with sub-pixel accuracy. Then, the gray code sequence is used to resolve ambiguities and determine uniquely the projector line number. An oversampling technique is used to make the ambiguity resolution more robust (Figure 6). In the next step the lines joining the detected stripe centers are intersected to obtain camera coordinates with sub-pixel accuracy for each projector coordinate.

The transition from the camera domain to the projector domain is one of the major differences between the two methods.

Performing the same steps for an arbitrary number of cameras, immediately gives us not only the correspondences between image points of a single camera / projector combination but also corresponding points between any of the cameras linked by a common projector.

3.2.4. Correction for Reflectance Discontinuities

Reflectance discontinuities on the object surface are a major source of errors for most 3-D sensors based on the evaluation of structured light patterns. In previous work, Curless and Levoy[8] have introduced *space-time analysis* to address this problem for a laser stripe range finder. Although we have successfully implemented space-time analysis for a stripe projection system, this means to establish correspondences between camera coordinates and sub-stripe projector coordinates. In consequence, we loose the direct link between different cameras seeing the same projector pattern. Thus we don't use it in a setup with an uncalibrated projector.

In contrast to laser stripe range finders, our system allows to acquire an "all-white" image of the work space. The information, gathered by this image and by a second image, containing only the effects of ambient lighting allows us to normalize the stripe images. This step considerably reduces the influence of reflectance discontinuities on the surface of the object.

For example, Figure 5 shows the effects of a strong surface intensity variation on the result of phase and line shift processing in a setup with a calibrated projector. The word "Intensity" is printed in black letters onto a white, planar surface. As a result, phase shift processing obtains height variations of up to 800 µm. Using line shift processing with intensity normalization, this can be reduced to 120 µm. It has to be noted that if we use line shift processing in combination with an uncalibrated projector, reflectance variations have less effect on the result, since all cameras are observing the same disturbed pattern, leading to correct correspondences.

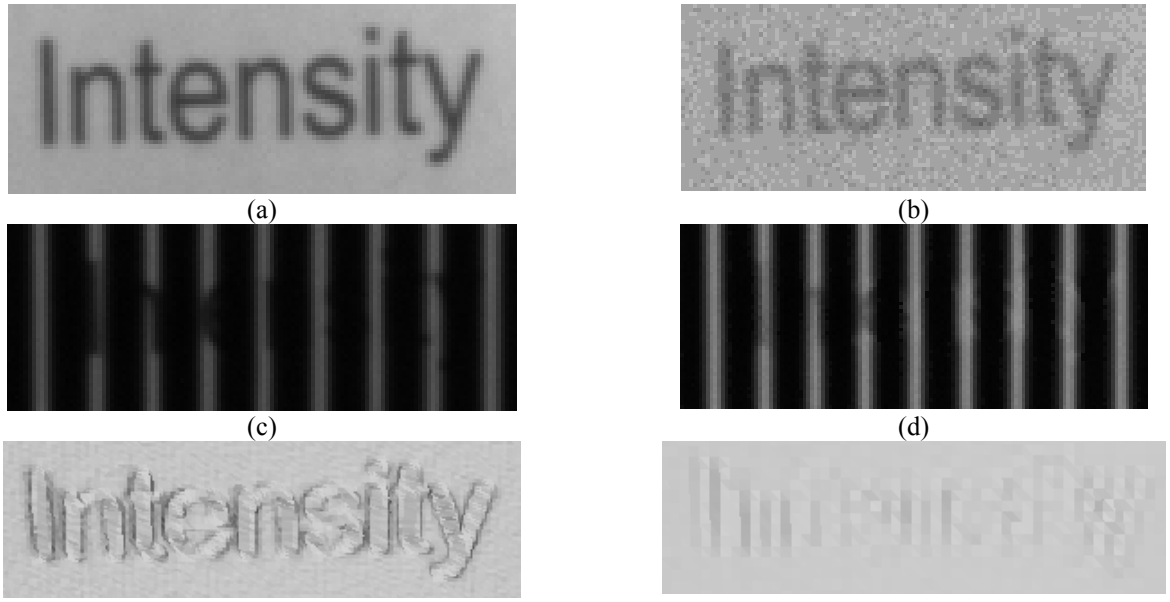

Figure 5. (a) Fully illuminated image. (b) Image without illumination by sensor (contrast enhanced). (c) Line shift image on a surface with high reflectance discontinuities. (d) Corrected line shift sequence. (e) Rendered view of the 3-D surface. The image coordinates have been obtained using phase shift processing. (f) Rendered view of the same extract using line shift processing.

3.2.5. Locating the Stripe Centers

A lot of research was done, mainly in the computer vision community, to efficiently determine the center of a light stripe with sub-pixel accuracy. Trucco et al.[6] compare five major algorithms. All of the considered algorithms determine the peak position by fitting a 1-D curve to a small neighborhood of the maximum of the stripe cross-section, assuming a Gaussian intensity profile. The algorithms are compared with respect to the bias introduced by the peak detector and the theoretical and practical behavior under ideal and noisy conditions. In summary, the results were that all but some small center of mass filters are reasonably unbiased and that a Gaussian approximation, developed by those authors, and two detectors developed by Blais and Rioux[7] performed well even under severe noise conditions.

Taking into account these results, we implemented our peak detection algorithm based on the detector of Blais and Rioux. After removing the effects of ambient lighting, the images are convolved by a fourth or eighth order linear filter:

$$g_4(i) = f(i-2) + f(i-1) - f(i+1) - f(i+2) \tag{4}$$

$$g_8(i) = f(i-4) + f(i-3) + f(i-2) + f(i-1) - f(i+1) - f(i+2) - f(i+3) - f(i+4) \tag{5}$$

We estimate the peak center position by linear interpolation at positions where a change in sign is encountered in the convolved image (Figure 6 (a)). This way, sub-pixel accuracy estimates for the peak center position are obtained.

3.2.6. Computing Image Space Coordinates

Once a peak center is detected, it is assigned the label (line number) of the projector line by which it was generated. Possible labels for the peak centers found in the n^{th} line shift image are the numbers $i \bmod n \; \forall \, i \in \{0, 1, \cdots, \#\text{PROJECTOR\_LINES} - 1\}$. In our case, n is in the range $0 \le n \le 5$ and the Gray code resolution is two projector lines yielding a region of three Gray code values matching one label. We hereby achieve an oversampling which makes the ambiguity resolution more robust. The labels are stored at the peak position in a set of label images, one image for each corresponding line shift image. We first sought to store all labels in one image per x and y coordinate, thus saving a lot of resources. However, using one label image

for each line shift image allows for the use of cameras with a lower resolution than the projector. The resulting label images contain connected chains of identical labels that look something like skeleton images of the stripe patterns. The sub-pixel locations of the stripe centers in the camera images are stored in the same manner.

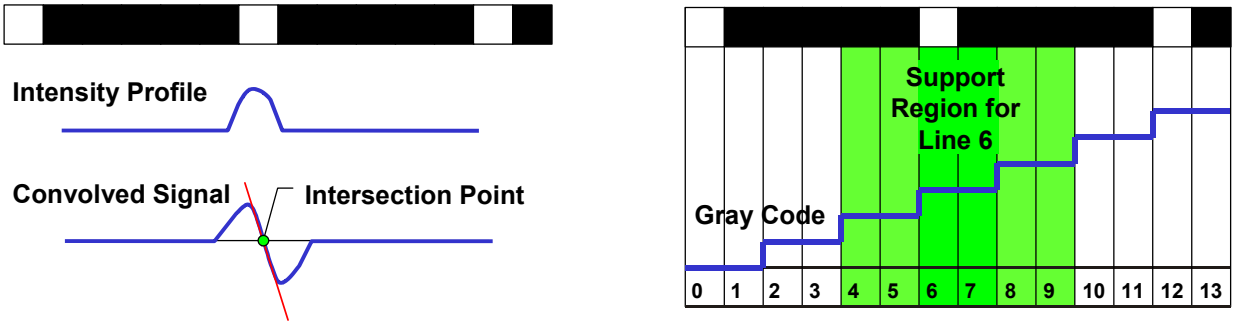

(a) (b)

Figure 6. (a) The sub-pixel position of the line center is detected by linear interpolation of the zero crossing in the convolved line shift image. (b) The distance between consecutive lines in one image is three times the resolution of the Gray code. The oversampling is used to establish support regions during the labeling process, yielding a more robust solution.

In the next step, a local operator is used to find any crossing between the center lines (the chains in the label images) of the label images for the horizontal and vertical sequence. The sub-pixel location of the crossing is found by intersecting two lines, connecting positions on either sides of the crossing.

The x and y coordinates of the intersection point are stored in images of the same size as the projector matrix. The transition from the camera domain to the projector domain is specific for our algorithm.

3.2.7. Computing Object Point Coordinates

3-D point determination is carried out using forward intersection based on the extrinsic and intrinsic parameters obtained from system calibration. Forward intersection uses a minimum of four observed image coordinates to estimate three world coordinates. Using more than two camera, redundancy and hereby accuracy and reliability can be significantly improved.

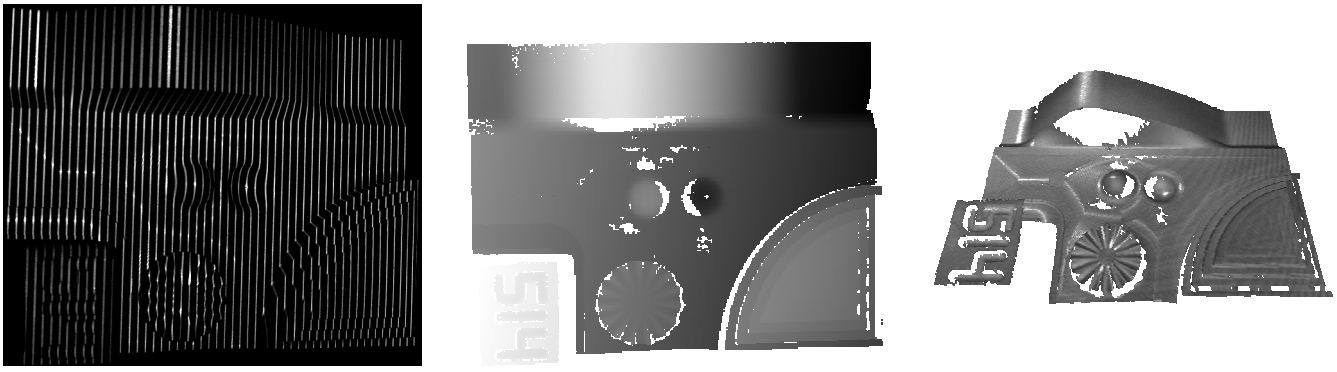

(a) (b) (c)

Figure 7. (a) One image of the *line shift* sequence. (b) Computed range image (z component). (c) Rendered view of the obtained surface. The holes are caused by points that have been eliminated by consistency checks, e.g. due to saturated pixels.

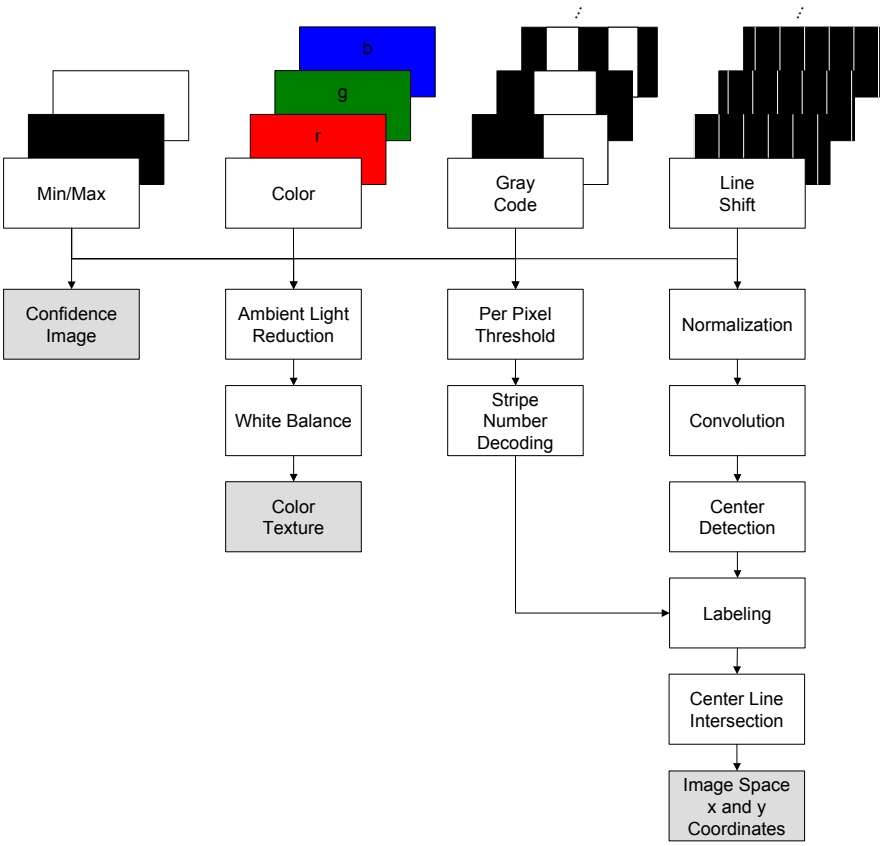

Figure 8. Flowchart of the Line Shift algorithm.

3.2.8. Improving Accuracy, Reliability and Consistency by use of multiple Cameras

Accuracy and reliability can be significantly improved if image data from multiple cameras is available, all sharing the same projector. Because line shift processing directly links projector lines to camera coordinates, corresponding pairs of image points between different cameras can easily be found. Each pair contributes four observations to solve for the three unknown object point coordinates. It is obvious, that a large number of observations, corresponding to a high redundancy, yields more accurate results.

In every case, object point coordinates are obtained by inverting a 3×3 matrix which afterwards contains the covariance information. Points that exhibit large residuals, as well as points seen at a steep angle can be removed.

The data, obtained by multiple cameras, can also be used to enforce explicit consistency tests. Specular reflections, as they are likely to occur on the surface of machined metal parts, cause spurious 3-D point measurements. The consistency tests are based on the observation, that specular reflections are viewpoint dependent. If the cameras view the object from different angles we can compute the deviation between object points, computed from different pairings of image points. This allows us to either discard one single observation or completely discard all the observations for the corresponding surface point.

3.2.9. Improving the visual Appearance: Intensity Information and Color Texture

The method described above allows us to capture the 3-D shape of objects represented as a set of images, one for the *X*, *Y* and *Z* coordinates in the sensor coordinate system. On the other hand there exist a large number of standard tools to visualize and explore 3-D data sets represented as quadrilateral or triangular meshes. The conversion into mesh representation is straightforward as the topology of the measured points is implicitly given by the position in the images. In addition, we can

use per vertex color or texture images to greatly improve the visual appearance. Although we are using monochrome cameras, registered color images can be obtained by projecting red, green and blue light on the object and capturing each individual color channel. Because of the non-uniform spectral sensitivity of the CCD-cameras, a white-balancing procedure has to be applied i.e. we scale the individual greyvalue images before merging them into one single RGB-image. In order to compute the scaling factors we acquire a white sheet of paper which must yield the same intensity for the red, green and blue color component.

3.2.10. Automating the Acquisition Process

A triangulation based measurement system can only capture those parts of an object that are visible by at least two cameras. The complete reconstruction of any non-trivial part makes it therefore necessary to measure the object from different viewpoints. Further processing allows us to register and integrate the datasets into a common surface description. Since registration is usually performed in an iterative manner the provision of initial values is inevitable.

The acquisition process can be automized using a computer controlled actuator. We are using a 3-axis positioning device to rotate the object and move it horizontally in two directions. This setup makes it easy to acquire surface information from different viewpoints while keeping the object in focus. Initial values for registration can be computed directly from the machine coordinates of the positioning device, thus speeding up the registration process.

4. SYSTEM CALIBRATION

4.1. Direct Calibration vs. Model Based Calibration

There are two basic approaches for the calibration of an optical 3-D system. *Direct calibration* uses an arbitrary calibration function (usually a polynomial) to describe the mapping from observations to three-dimensional coordinates. The parameters of this function are obtained by measuring a large number of well-known points throughout the measuring volume. An immediate advantage is, that no care has to be taken to model any phenomena, since every source of error is implicitly handled by the computed coefficients.

However, direct calibration requires a highly accurate calibration normal. Especially for sensors with a large measurement volume, as in our case, this requirement complicates the calibration procedure or makes it even impossible. Since the calibration function acts as a black box, there is no information about the quality of measurements.

In *model based calibration*, parameters of a geometric model of the sensor, so called intrinsic and extrinsic parameters, are determined. The model describes how points in 3-D space are projected onto the image plane, considering imperfect cameras and lenses. There exist techniques in photogrammetry to simultaneously estimate these parameters during measurement tasks, however, most commonly a specially designed test object is used to effectively compute the desired quantities from a few calibration measurements. Since any short-term geometrically stable object can be used for calibration, there is no need for an accurate calibration normal. Nonetheless, if absolute measurements are required, at least one accurate distance (e.g. from a scale bar) is needed to fix the scale.

On the down side, highly accurate measurements require complicated sensor models and some effects in the image formation process might remain uncorrected.

In a previous paper (Brenner et al., 1999) we have compared polynomial depth calibration, a standard direct calibration technique to model based photogrammetric calibration. As a conclusion, we found that both calibration procedures yield comparable accuracies. However, in our opinion it is advantageous to obtain the model parameters explicitly. The fact, that model parameters hold true for all the measurement volume of the sensor omits problems with measurements lying outside the volume originally covered by calibration. In addition, residuals and the covariance matrix give a clear diagnosis for the determination of the calibration parameters and object point coordinates.

4.2. Photogrammetric Calibration

Since we use a standard stereo or multi camera setup, the system can be calibrated using a planar test field and a convergent setup. Our test field consists of an aluminum plate, on which we fixed a sheet of self-adhesive paper showing white dots on a black background. Five of those targets are surrounded by white rings. These rings allow to determine the orientation of the test field. In the next step all visible target points are measured and identified fully automatically. Then, image coordinates for the camera are obtained by computing the weighted centroid. These measurements are used to compute the bundle solution for the calibration parameters externally using the "*Australis*" software package from *The Department of Geomatics* of *The University of Melbourne*. Our camera is modeled with 10 parameters, namely the focal length c, the principal point offsets Δx and Δy, K_1, K_2 and K_3 for radial symmetric distortion, P_1, P_2 for decentering distortion and finally B_1 and B_2 for scale and shear[10].

4.3. Actuator Calibration

Actuator calibration is necessary to link the coordinate system of the positioning device to the sensor coordinate system. While surface measurements require a high degree of accuracy, the calibration of the positioning device is only needed to provide initial values for the registration process. We therefore decided to implement a very simple calibration procedure. It uses a little adapter featuring a plate with two white target points on black background. The adapter fits precisely into a hole in the center of the rotary table. The mechanical assembly hereby guarantees that both target points lie exactly in the axis of rotation. The 3-D positions of the target centers are determined by the measurement system. In the next step, we move the actuator in direction of the first linear axis and measure the targets again. This step is repeated for the second linear axis. We now have a reference position and the directions of all three axes. Hence we can compute for any movement of the positioning device the corresponding transformation of the sensor coordinate system.

5. EXPERIMENTAL RESULTS

This section reports some tests to assess the performance of the measurement system. The first test uses a granite reference plane as a calibration normal. The plane is certified to have an overall surface flatness of 7 microns. Since the surface is black, we covered it with a self-adhesive white foil to obtain a high signal modulation. The reference plane was positioned in front of the sensor. The overall measurement area was about $700\times500\,mm^2$ but we only used a $200\times200\,mm^2$ portion, located in the corner of the measurement area where the largest errors can be expected. A plane is fitted to the measured 3-D points and minimum, maximum and standard deviation from the plane are determined.
Table 1 shows the result of this step, obtained using the LCD and the DMD projector. This translates to approximately 1:20,000 relative accuracy.

Type of Projector	Standard Deviation [mm]	Maximum Deviation [mm]	Structure
LCD	0.030	0.281	moirés
DMD	0.028	0.127	regular, vertical lines

Table 1. Deviation of measured 3D points from a fitted plane.

It is interesting that the deviations show a characteristic pattern for each of the two projectors. Small gaps around the pixels of the LCD projector cause a visible dark grid that interferes with the pixel structure of the CCD, resulting in moiré patterns in the deviation image. For the measurements of the DMD projector the deviations show a periodic pattern in horizontal direction (Figure 9).

For the second test a specially designed 3-D test part has been measured (Figure 7). The part was intended to provide a number of features that can help to evaluate the quality of the acquired data. The qualitative analysis shows good results featuring a lot of details, although the large planar region shows a similar pattern as in the first test.

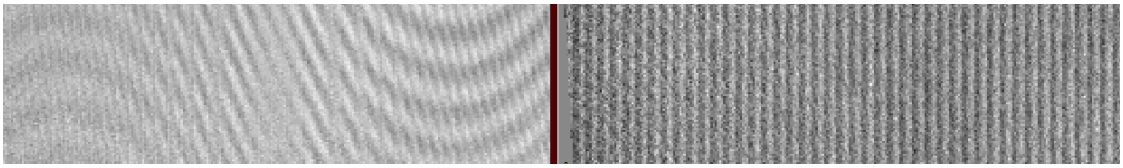

Figure 9. Deviation from the best fitting plane for the LCD set up (left) and the DMD set up (right).

6. CONCLUSIONS

A coded light measurement system based on the combination of monochrome cameras with a multimedia projector was presented. The system provides a large measurement area and high accuracy. In addition, registered color information can be acquired and used to enhance the visual appearance for visualization purposes.

Calibration of the intrinsic and extrinsic parameters of the cameras was achieved using well-known photogrammetric techniques.

To overcome the limitations of conventional phase shift processing, an alternative processing scheme, called *line shift processing*, was developed and explained in detail. An immediate advantage of the new method is the transition from the camera domain to the projector domain, linking integer-valued projector coordinates to sub-pixel camera coordinates. Thus, correspondences between multiple cameras in a single projector, multiple camera setup can easily be established. If more than two cameras are available, correspondences between multiple cameras can considerably improve accuracy and allow to define explicit consistency criteria in order to reject spurious measurements.

The accuracy of the new method has been investigated by measuring a highly accurate reference plane. As a result, we can state that under ideal conditions the system provides a relative accuracy of about 1:20,000.

ACKNOWLEDGMENTS

The support of the German Research Foundation under research grant DFG-SFB514 is gratefully acknowledged. We also thank the Department of Geomatics, The University of Melbourne, for providing us the Australis software package and Claus Brenner, the former head of our group, for the introduction to the field of photogrammetry and computer vision, his support and friendship.

REFERENCES

1. M. Altschuler, B. R. Altschuler, J. Taboada, “Measuring surfaces spacecoded by a laser-projected dot matrix”, *Imaging Applications for Automated Industrial Inspection and Assembly ,* **182**, SPIE , 1979.
2. T. G. Stahs, F. M. Wahl, “Fast and robust range data acquisition in a low-cost environment”, *Close-Range Photogrammetry meets Machine Vision*, **1395**, SPIE, pp. 496-503, 1990.
3. J. Gühring, C. Brenner, J. Böhm, and D. Fritsch, “Data Processing and Calibration of a Cross-Pattern Stripe Projector”, *International Archives of Photogrammetry and Remote Sensing* **33**, Part B5/1, pp. 327-338, Amsterdam, 2000.
4. J.-M. Bofinger, “Dichte dreidimensionale Oberflächenerfassung mittels Streifenprojektion unter Verwendung von Standardkomponenten“, *Seminar Thesis, Institute for Photogrammetry (ifp)*, Stuttgart, Germany, 2000.
5. MICO website: http://www.mico.org
6. E. Trucco, R. B. Fisher, A. W. Fitzgibbon, D. K. Naidu,. “Calibration, data consistency and model acquisition with laser stripers”, *Int. J. Computer Integrated Manufacturing*, **11**, No. 4, pp. 293-310, 1998.
7. F. Blais, M. Rioux, “Real-time numerical peak detector”, *Signal Processing* **11**, pp. 145-155, 1986.
8. B. Curless, M. Levoy, “Better optical triangulation through space-time analysis”, *Proc. IEEE Conf. on Computer Vision (ICCV)*, pp. 987-994 1995.
9. C. Brenner, J. Böhm, J. Gühring,. “Photogrammetric calibration and accuracy evaluation of a cross-pattern stripe projector”, *Videometrics VI* **3641**, SPIE, San José, CA, pp.164-172, 1999.
10. C. S. Fraser,. “Digital camera self-calibration”, *ISPRS Journal of Photogrammetry and Remote Sensing*. **52**, No. 4, pp. 149-159, 1997.